

AN1026

1/f Noise Characteristics Influencing Phase Noise

Abstract

In applications such as VCO's where 1/f noise is one of the major contributors to phase noise, the device with the best 1/f noise will yield the best phase noise. To better understand how 1/f noise changes with bias and from device to device, the 1/f noise of two different bipolar devices were measured and compared. Nonlinear models were developed and the predicted and measured 1/f noise spectrums compared. In addition, how manufacturers quantify 1/f for simulation purposes is evaluated to provide the designer who is new to noise simulation with better insight into what the 1/f coefficient and exponent mean, and how the values effect the 1/f noise simulations.

I. Introduction

The phase noise of an oscillator, quantified by its short term frequency stability, determines a system's ability to separate adjacent channels. With the significant increase in portable, wireless traffic, better frequency stability is required. Phase noise becomes an important consideration. Choosing the appropriate topology for a low phase noise source is important, as is the choice of resonator and coupling network [1]. Many articles exist on how to design an oscillator for low phase noise by selecting the appropriate topology, resonator and coupling network[2]. This article focuses on the important characteristics for *device* evaluation and selection.

II. Oscillator Phase Noise

Phase perturbations due to random noise in the oscillator result in a random shift of the oscillator frequency. These random frequency variations are caused by thermal noise, shot noise, and flicker noise. Thermal noise is a function of the temperature, bandwidth and resistance, shot noise is a function of the DC bias current, and flicker noise is a function of the active device characteristics. Single sideband phase noise is defined as the noise power in a 1-Hz bandwidth at some offset frequency from the carrier, F_{osc} , and has the units of dBc/Hz, Figure 1.

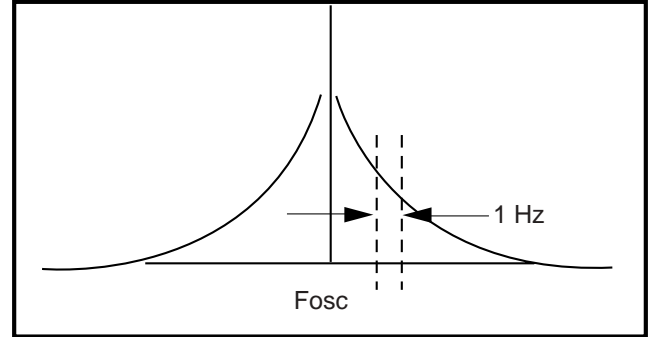


Figure 1. Single sideband phase noise

Oscillator phase noise has two components: phase noise resulting from direct upconversion of white noise and 1/f noise, and phase noise resulting from the changing phase of the noise sources modulating the oscillation frequency, Δ freq. The composite oscillator phase noise spectrum consists of the white noise and 1/f noise directly upconverted around the carrier, and the phase modulated noise spectrum. The frequency noise in the frequency domain is converted to phase noise in the frequency domain by multiplying by $1/f^2$. The white noise spectra, f^0 , then contributes $1/f^2$ and the 1/f noise spectra contributes $1/f^3$, see Table 1.

Noise Source	Phase Noise Spectrum	
	Upconverted	Δ freq
white noise	white noise	$1/f^2$
1/f noise	1/f noise	$1/f^3$

Table 1. Noise sources and their phase noise spectrum

For a low Q oscillator where the half-bandwidth frequency, $f_o/2Q$, is greater than the flicker corner frequency, f_c , the oscillator phase noise characteristics will be determined by the white noise, $1/f^2$, and the flicker noise, $1/f^3$, Figure 2.

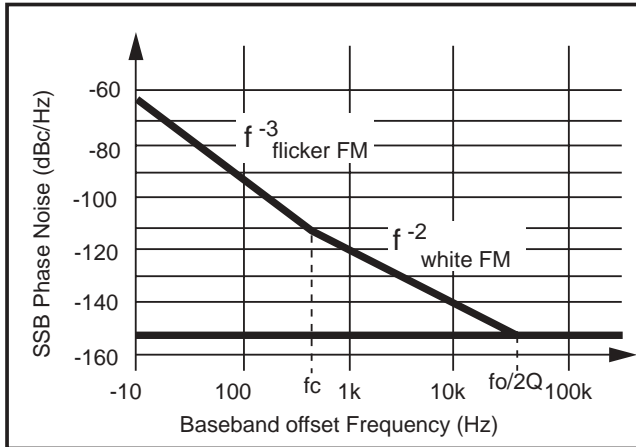


Figure 2. Baseband noise spectrum for $f_c < f_o/2Q$, Low Q.

For a high Q oscillator where the halfbandwith frequency, $f_o/2Q$, is less than the flicker corner frequency, f_c , the oscillator phase noise characteristics will be determined by the frequency modulated flicker noise, $1/f^3$, and the upconverted $1/f$ noise, Figure 3.

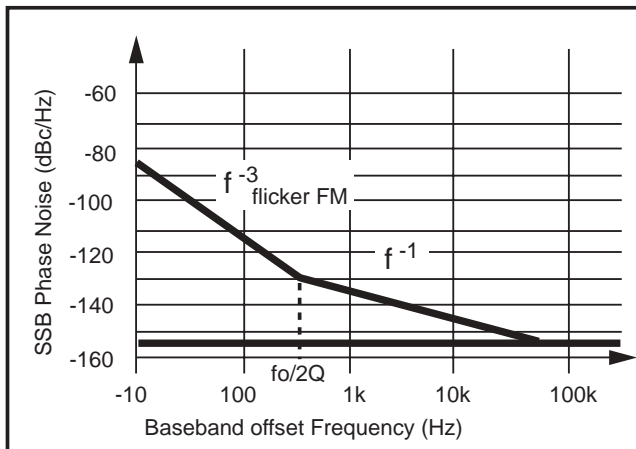


Figure 3. Baseband noise spectrum for $f_c > f_o/2Q$, High Q.

III. 1/f Measurements

1/f measurements are performed to obtain the flicker noise frequency spectra and determine the flicker corner frequency. From this spectra, the simulation coefficient KF and the simulation exponent AF necessary for modeling the 1/f noise spectra can be determined.

Flicker noise in BJTs is also known as 1/f noise because of the 1/f slope characteristics of the noise spectra. This noise is caused mainly by traps associated with contamination and crystal defects in the emitter-base depletion layer. These traps capture and release carriers in a random fashion. The time constants associated with the process produce a noise signal at low frequencies. The flicker noise spectral density is given by:

$$S(f)df = (KF)IB^{AF}df / Fc \tag{1}$$

where:

- KF = flicker noise constant
- AF = flicker noise exponent
- IB = DC base current
- Fc = flicker noise corner frequency

A. Noise Test Setup

The test setup to measure 1/f noise is shown in Figure 4. The 50 ohm terminations insure amplifier stability at higher frequencies. The entire test setup is contained in an EMI shielded box. The supply voltages, VBB and VCC are provided by batteries to eliminate 60 Hz noise.

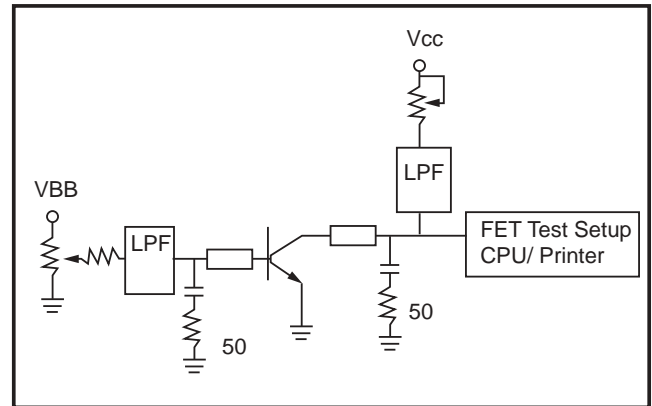


Figure 4. 1/f Noise Test Setup

The measured 1/f noise spectrum for the NE68819 at $V_{ce} = 3V$, $I_c = 12mA$ is shown in Figure 5. The measured flicker corner frequency, $F_{meas} = 5.6kHz$, is determined by noting the intersection of the 1/f noise spectrum and the white noise spectrum. This intersection is where the measured flicker noise power and the white noise power are equal.

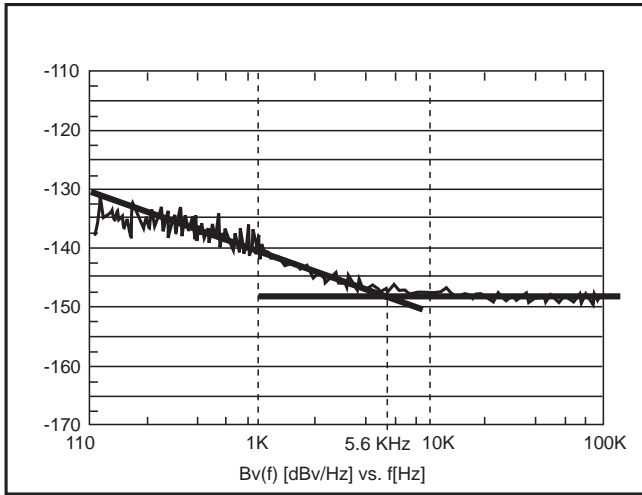


Figure 5. 1/f measurement for the NE68819 at Vce=3V, Ic=12 mA

To determine the intrinsic base flicker noise corner, F_{bn} , requires solving the following equation [3]:

$$F_{bn} = F_{meas} [1 + 1/\beta + 2V_{th}G_{in}/IB] \quad (2)$$

where:

- F_{bn} = intrinsic base flicker noise corner
- F_{meas} = measured flicker corner
- β = collector-base current gain
- V_{th} = thermal voltage = kT/q
- G_{in} = external input conductance
- IB = DC base biasing current

The equation for the intrinsic base flicker corner modifies the measured flicker corner to account for the input conductance, base current, and DC current gain of the device. The formula for F_{bn} is valid providing the measured output noise characteristics are dominated by the base flicker and base shot noise sources. The design of the test setup and selection of biasing circuitry is chosen to insure these conditions.

B. Calculating AF and KF

Measuring the flicker corner frequency at two different base currents provides two different flicker corner values. Using equation (3) twice, once for each IB and F_{bn} value provides two equations and two unknowns, resulting in a solution for AF and KF.

$$F_{bn} = (KF)IB^{(AF-1)} / 2q \quad (3)$$

The resulting expressions for AF and KF are:

$$AF = \frac{\log(F1) - \log(F2) + Z}{Z} \quad (4)$$

$$Z = \log(IB1) - \log(IB2)$$

$$KF = 10 (\log(F_{bn}) + \log(IB) - 18.49 - (AF)\log(IB)) \quad (5)$$

Calculated AF and KF values resulting from 1/f measurements for the NE68519 and the NE68819 are provided in Table 2.

Ic (mA)	NE68519				NE68819			
	VCE=1V		VCE=3V		VCE=1V		VCE=3V	
	AF	KF	AF	KF	AF	KF	AF	KF
5	1.56	454	1.35	80	1.9	5	1.18	10
10	1.48	231	1.19	18	1.39	72	1.22	15
20	1.89	7.6K	1.12	13	1.19	14	1.23	16
30	1.6	774	1.25	30	1.16	10	1.26	26

Table 2. AF and KF for the NE68519 and the NE68819 (KF values are times 10^{15})

C. Bias Dependency

Next we examine the bias dependency of the flicker corner frequency for the same two NEC devices. The base voltage was varied to obtain the collector currents shown in Table 3. The flicker corner frequency, F_{bn} , was determined at VCE=1V and VCE=3V as shown in Table 3 and Figure 6.

Ic (mA)	Fbn (KHz)			
	NE68519		NE68819	
	Vce=1V	Vce=3V	Vce=1V	Vce=3V
5	5.8	7.3	5.6	5.1
10	8.8	9.9	5.9	5.8
20	12.4	11.2	7.7	6.7
30	18.6	11.9	8.3	7.3

Table 3. F_{bn} versus bias - NE68519, NE68819

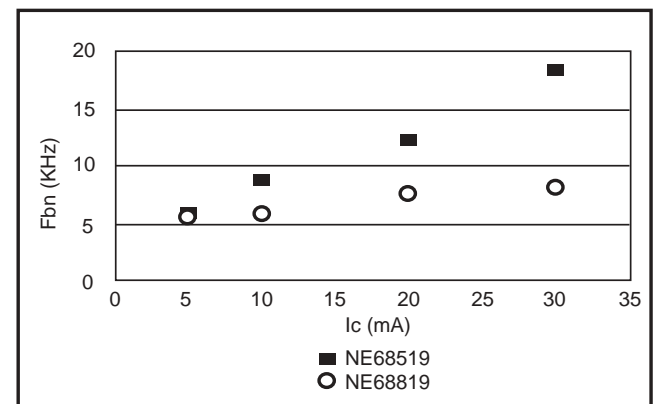


Figure 6a. F_{bn} at VCE=1V for the NE68519 and the NE68819

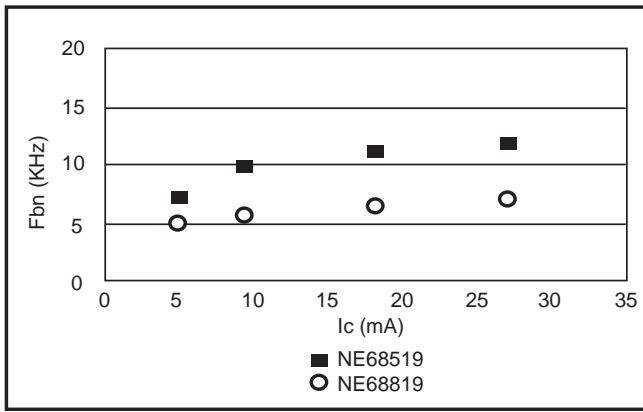


Figure 6b. F_{bn} at $V_{ce}=3V$ for the NE68519 and the NE68819

The flicker corner frequencies for the two devices are within 3% at the lower bias of $V_{ce}=1V$ and $I_c=5mA$; $F_{bn}=5.8kHz$ for the NE68519 and $F_{bn}=5.6kHz$ for the NE68819. At higher biases, the NE68819 has lower $1/f$ noise.

As the bias voltage increases from 1V to 3V with a constant collector current $I_c=20mA$, the amplitude of the $1/f$ slope is unchanged but the amplitude of the white noise floor increases due to the increase in thermal noise voltage as shown in Figure 7a. The higher noise floor results in a lower $1/f$ corner frequency of 11.8kHz at $V_{ce}=3V$. At $V_{ce}=1V$ the $1/f$ corner frequency is 16kHz.

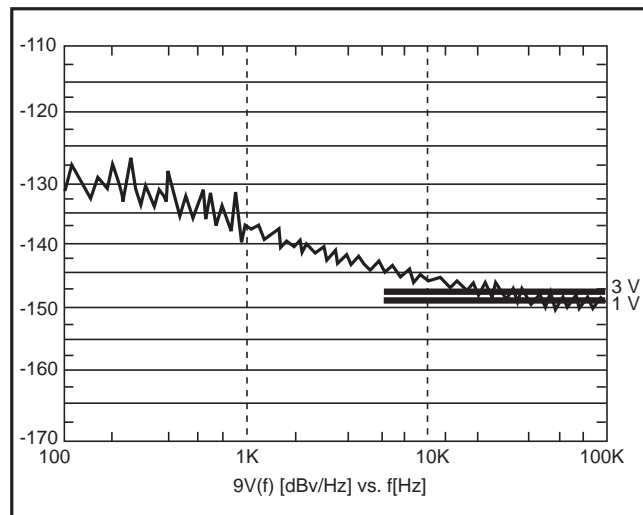


Figure 7a. $1/f$ measurement with I_c constant, $I_c=20mA$ and $V_{ce}=1V$ and $3V$ for the NE68519

As the bias current increases from 5mA to 10mA and the bias voltage stays constant at $V_{ce}=3V$, the $1/f$ spectrum amplitude increases proportionally with increases in base current, and the shot noise component of the white noise floor increases proportionally with increasing base current, Figure 7b.

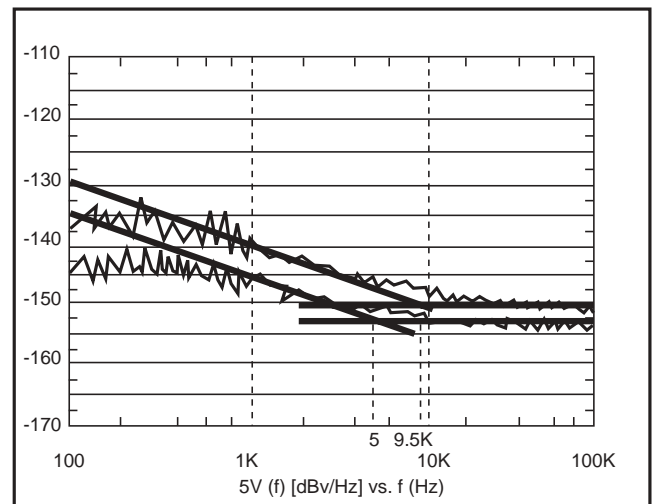


Figure 7b. $1/f$ measurement with V_{ce} constant, $V_{ce}=3V$, and $I_c=5mA$ and $10mA$ for the NE68519

IV. $1/f$ Noise Simulation

A nonlinear model was developed for the NE68519 and the NE68819. The simulation schematic and the variable values for the NE68819 are shown in Figures 8a and 8b. The simulator used is the LIBRA™ harmonic balance simulator by HP/EESOF [4]. The test bench is shown in Figure 8c. Note that $AF=1.26$ and $KF=2.6e-14$ to provide flicker noise simulation. Simulated $1/f$ noise for the NE68819 at $V_{ce}=3V$, $I_c=10mA$ is shown in Figure 9.

A. NE68819 simulated versus measured

Measured $1/f$ noise spectra at $V_{ce}=3V$, $I_c=12mA$, Figure 5, was compared to simulated $1/f$ noise at $V_{ce}=3V$, $I_c=10mA$, Figure 9. Although the collector currents were 20% different, the $1/f$ corner frequencies - measured vs model - were within 10% of each other. The white noise floor was $-149dB$ (measured) compared to $-151dB$ (model) resulting in a 1.32% difference. The 1MHz noise amplitude was $-131dB$ (measured) compared to $-132dB$ (modeled), a difference of only 0.76%.

B. Modeling $1/f$ noise with AF and KF

Most commercial simulators set AF and KF to default values of 1.0 and 0 respectively. Inspection of equation (1) shows that if $KF=0$, the flicker noise spectral density will also be 0, resulting in the presence of white noise only. Examining figure 10c with $KF=1e-13$ shows the $1/f$ spectra approaching the white noise spectra. Figures 10a and 10b model the $1/f$ spectra changes as KF and AF are varied. Note that the Y-intercept of the $1/f$ spectra increases proportionally to KF, as expected from equation (1). The Y-intercept of the $1/f$ spectra decreases more rapidly with increases in AF. Equation (2) verifies this to be the case with the $1/f$ spectral density decreasing exponentially with increases in AF, since IB is less than unity.

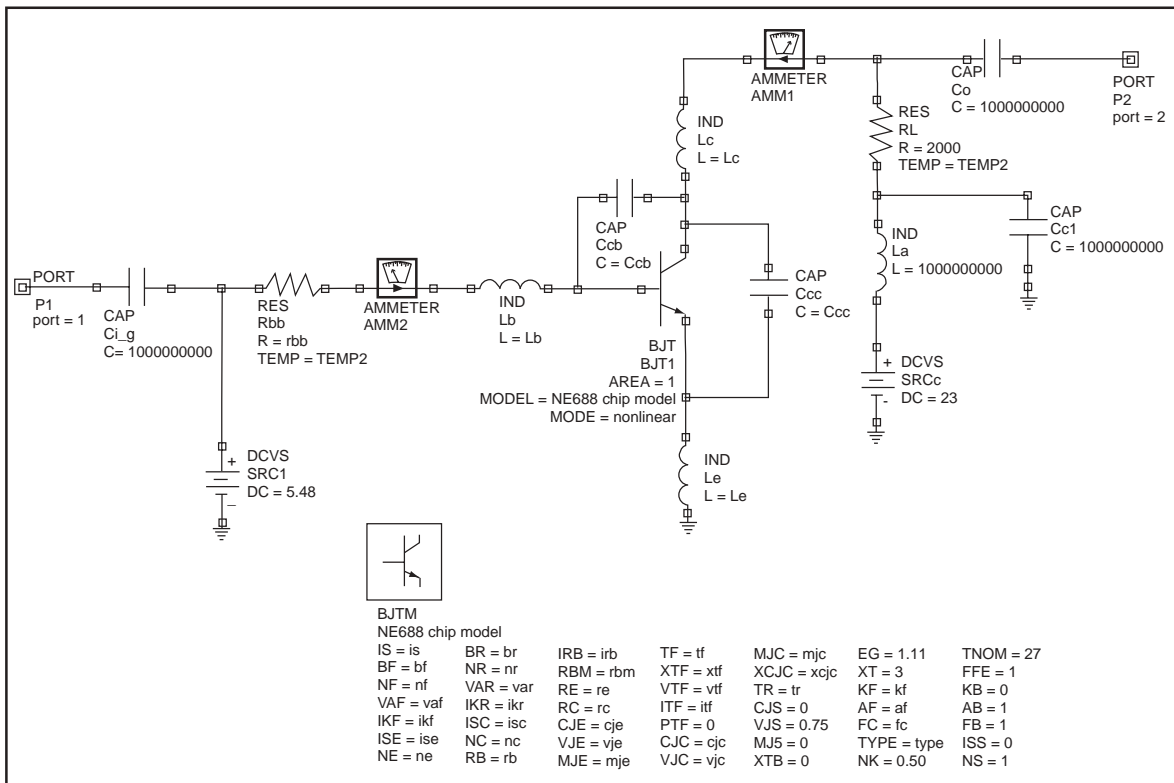


Figure 8a. NE68819 Simulation Schematic

<p>UNITS</p> <p>UNITS_DEFAULT</p> <p>FREQ=GHz</p> <p>RES=ohm</p> <p>COND=S</p> <p>IND=nH</p> <p>CAP=pF</p> <p>LNG=mil</p> <p>TIME=psec</p>	<p>ANG=deg</p> <p>POWER=dBm</p> <p>VOLT=V</p> <p>CUR=mA</p> <p>DIST=mi</p>	<p>DATA</p> <p>TEMP</p> <p>TEMP_DEFAULT</p> <p>TEMP=27</p>	<p>DATA</p> <p>RREF</p> <p>RREF_DEFAULT</p> <p>R=50</p>	<p>DATA</p> <p>TAND</p> <p>TAND_DEFAULT</p> <p>TAND=0</p>	<p>DATA</p> <p>SIGMA</p> <p>SIGMA_DEFAULT</p> <p>SIGMA=0</p>	<p>DATA</p> <p>PERM</p> <p>PERM_DEFAULT</p> <p>MUR=1</p> <p>TANM=0</p>
<p>Var</p> <p>Eqn</p> <p>_VAR</p> <p>is=3.80e-16</p> <p>br=12.28</p> <p>nr=1.10</p> <p>bf=135.70</p> <p>var=3.50</p> <p>nf=1.00</p> <p>ikr=0.06</p> <p>vaf=28</p> <p>ikf=0.60</p> <p>isc=3.50e-16</p> <p>ise=3.80e-15</p> <p>ne=1.49</p> <p>rb=6.14</p>	<p>irb=1.00e-03</p> <p>rbm=3.50</p> <p>re=0.40</p> <p>rc=4.20</p> <p>cje=7.96e-13</p> <p>vje=0.71</p> <p>mje=0.38</p>	<p>tf=1.10e-11</p> <p>xtf=0.36</p> <p>vtf=0.65</p> <p>itf=0.61</p> <p>ptf=50</p> <p>cjc=5.49e-13</p> <p>vjc=0.65</p>	<p>mjc=0.48</p> <p>xcjc=0.56</p> <p>tr=3.20e-11</p> <p>fc=0.75</p> <p>kf=2.60e-14</p> <p>cf=1.26</p> <p>Ccb=0.24</p>	<p>Cce=0.27</p> <p>xcjc=0.56</p> <p>tr=3.20e-11</p> <p>fc=0.75</p> <p>kf=2.60e-14</p> <p>cf=1.26</p> <p>Ccb=0.24</p>	<p>Cce=0.27</p> <p>Lb=0.72</p> <p>Lc=0.51</p> <p>Le=0.19</p> <p>rb=50000</p>	
<p>NE688_chip_model PARAMETERS AND BONDING PARASITICS</p> <p>DATE: 10/2/96</p> <p>PROJECT NAME: 68800</p> <p>LIBRA DEFAULT FILE: 68800_def</p>						

Figure 8b. NE68819 nonlinear model parameter values

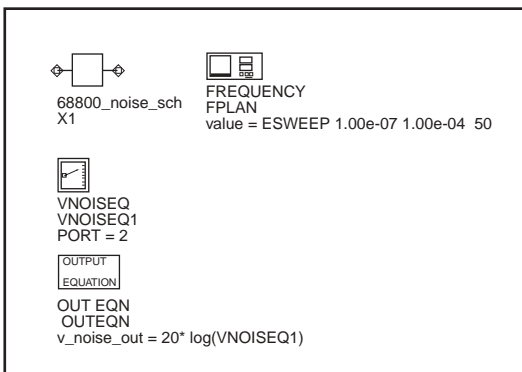


Figure 8c. NE68819 test bench

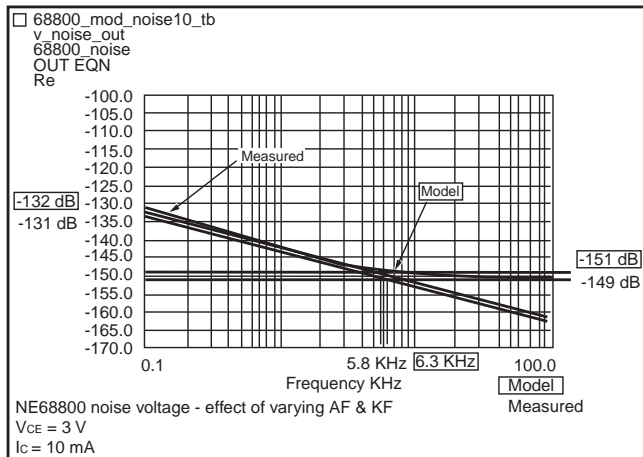


Figure 9. 1/f noise simulation for the NE68819 at $V_{ce}=3V, I_c=10mA$

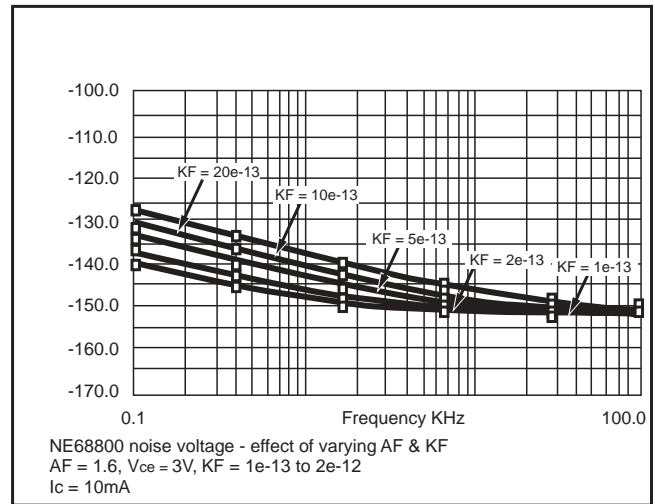


Figure 10c. Effect of varying KF from $1e-13$ to $20e-13$ with $AF=1.6$

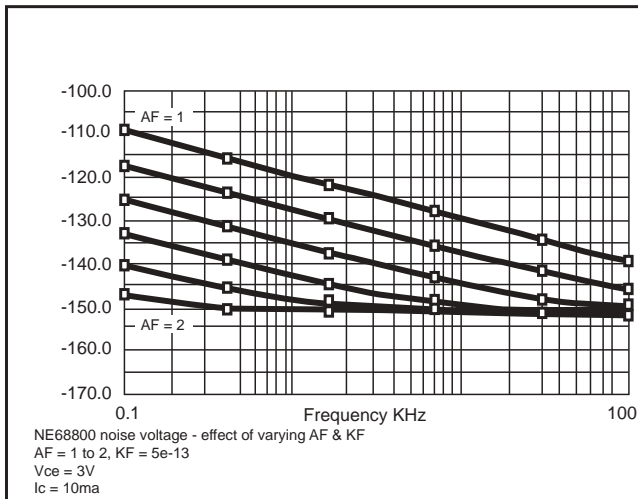


Figure 10a. Effect of varying AF from 1 to 2 with $KF=5e-13$

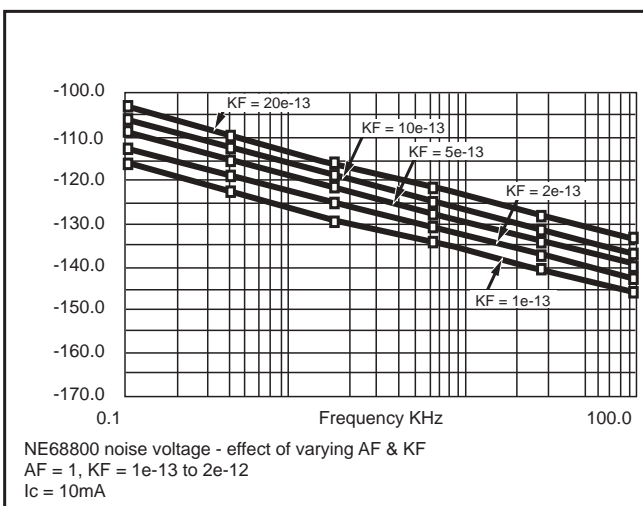


Figure 10b. Effect of varying KF from $1e-13$ to $20e-13$ with $AF=1$

CONCLUSIONS

1. Using the test setup and measurement techniques described, 1/f noise can be measured.
2. Using an accurate nonlinear model, 1/f noise simulations agree closely to measured data.
3. As V_{ce} increases, the flicker corner increases as the white noise increases, but the magnitude of the 1/f noise is constant.
4. As base current increases, the flicker corner frequency increases with the magnitude of the 1/f noise and the increased shot noise current.
5. 1/f noise increases linearly as KF increases and decreases with increases in AF for IB less than 1.0 amp, as is expected from equation (1).

REFERENCES

[1] Roger Muat, "Choosing devices for quiet oscillators", Microwave & RF, August 1984, pp. 166-170.
 [2] Grant Moulton, "Dig for the roots of oscillator noise", Microwave & RF, pp. 65-69, April 1986.
 [3] Julio Costa et al, "Extracting 1/f Noise Coefficients for BJT's," IEEE Transactions on Electron Devices, Vol. 41, No.11, pp. 1992-1999, Nov. 1994
 [4] "Simulating Noise in Nonlinear Circuits Using the HP Microwave and RF Design Systems," HP Product note 85180-4, c 1993.

California Eastern Laboratories

Exclusive Agents for NEC RF, Microwave and Optoelectronic semiconductor products in the U.S. and Canada

4590 Patrick Henry Drive, Santa Clara, CA 95054-1817
 Telephone 408-988-3500 • FAX 408-988-0279 • Telex 34/6393
 Internet: <http://WWW.CEL.COM>

Information and data presented here is subject to change without notice. California Eastern Laboratories assumes no responsibility for the use of any circuits described herein and makes no representations or warranties, expressed or implied, that such circuits are free from patent infringement.